Paper pa17-025
Submitted to the 28th International Conference on High Energy Physics
ICHEP'96, Warsaw, Poland, July 1996

The Forward Proton Spectrometer of H1

H1 Collaboration

Abstract

Since 1995 the H1 experiment at HERA is operating a forward proton spectrometer (FPS) employing the HERA machine magnets adjacent to the interaction zone as spectrometer magnets. Scattered protons are detected in two stations 81 and 90 m behind the interaction point with scintillating fiber hodoscopes. The experimental set up, the performance of the spectrometer and the technique to reconstruct proton momenta are described. A typical momentum resolution of 4 GeV at 650 GeV has been achieved with a scale uncertainty estimated to be 3%. All numbers presented in this paper are preliminary.

1 Introduction

At the HERA collider facility a class of events is observed in deep inelastic electron proton scattering and photoproduction, which is characterised by the absence of secondary particles in a region of phase space between the outgoing proton debris and the target jet. These so called rapidity gap events have all features of diffractive interactions known from hadron–hadron scattering. Thus it is expected that in a fraction of these events the proton stays intact and leaves the interaction point unobserved through the beam pipe. In order to detect them the HERA machine magnets adjacent to the interaction region are employed in a proton spectrometer. After about 80 m protons, which are emitted at angles less than 0.5 mrad with respect to the beamline and have lost more than 5% of their energy, appear at a distance of several millimeters from the nominal orbit so that they can be registered in detectors close to the circulating proton beam.

A permanent installation of counters a few millimeters from the proton beam is not possible, because they would cut into the machine aperture needed for injection and acceleration. The detector elements are thus mounted inside movable vacuum sections, so called Roman Pots, which are retracted during injection and are brought close to the beam after stable conditions have been reached. Fig. 1 shows a sketch of such a Roman Pot device with detectors and housing for front end electronics.

During the 1995 running period the H1 group operated two Roman Pots at 81 and 90 m with scintillating fiber hodoscopes to measure the position and direction of scattered protons, which is sufficient to reconstruct their angle and momentum at the interaction point. A data sample of about 2.6 pb^{-1} has been accumulated.

2 Forward Proton Spectrometer (FPS) Set Up

The HERA beam line is sketched in Figure 2. It provides a horizontal bend of the proton beam by dipoles around 20 m and a vertical deflection by three dipole magnets between 60 and 80 m. Also indicated are the positions of the two detector stations at 81 and 90 m, which serve to reconstruct trajectories of scattered protons.

Due to the fact that the HERA beam line introduces a dispersion in two planes, longitudinal momenta can be measured twice by making use of the horizontal and vertical deflections. The two independent measurements which have to agree within errors, if they belong to a track starting at the interaction point, enable a self calibration of the forward spectrometer and provide efficient means to reject background tracks. The detectors inside the Roman Pot plunger vessels thus have to record two coordinates (x horizontally and y vertically) at two positions behind the interaction region such that a straight line through the measured space points determines a trajectory which can be traced back to the origin by employing the known transfer properties of the magnetic channel.

The detector units for measuring space points at 81 and 90 m are sketched in Figure 3. Each station is equipped with two identical subdetectors consisting of two planes of scintillating fiber hodoscopes with u and v orientation ($\pm 45^0$ tilt angle) sandwiched between two planes of trigger scintillators. Four of the 1 mm diameter scintillating fibers belonging to a read out plane are attached to one cell of a 64 pixel position sensitive

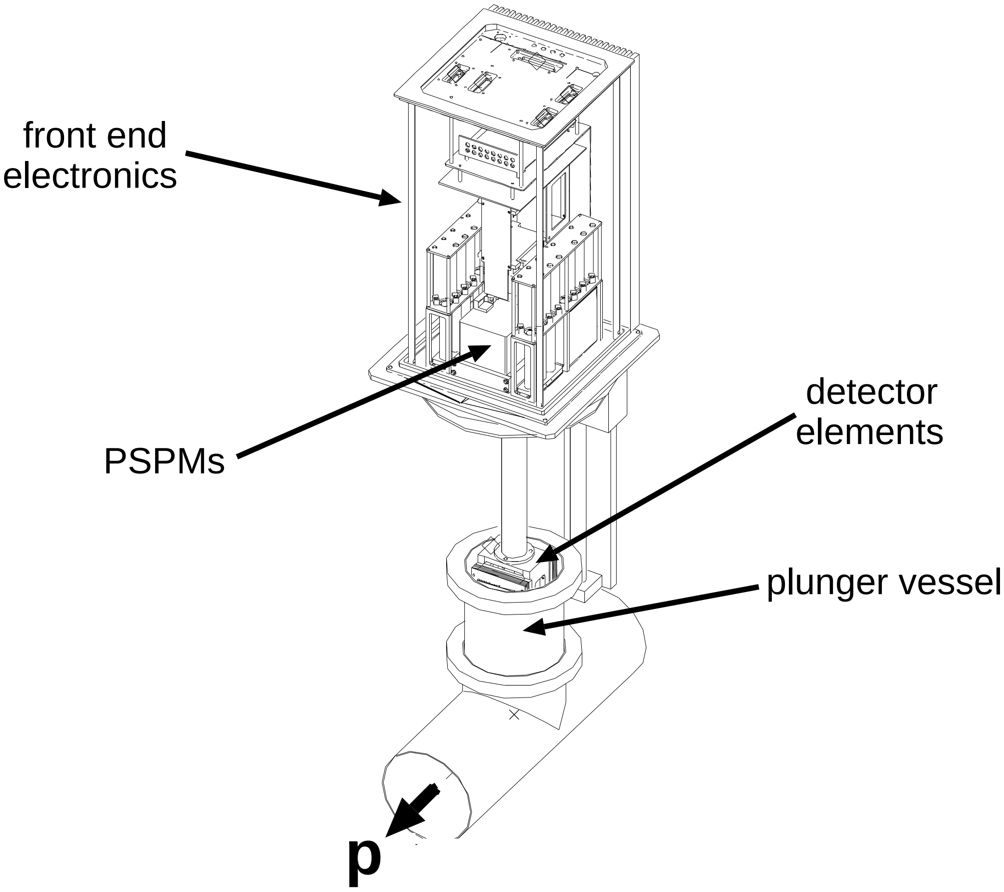

Figure 1: Scematics of a Roman Pot device for a scintillating fiber hodoscope detector.

Fiber hodoscopes	
Fibers per coordinate and subdetector	5 layers with 48 fibers
Total material thickness per station	$24\,mm \simeq 5.68\,\%\,X_0 \simeq 3.0\,\%\,\lambda_I$
Fiber diameter	1.00 mm
Fiber type	POLHITECH 042–100
Staggering	0.21 mm
Layer efficiency	$60 - 75\,\%$
PSPMs	
Type	Hamamatsu 4139–20
Number of pixels	64
Pixel size	$\varnothing 4\,mm$
Amplification at 2 kV	$3 \cdot 10^6$
Quantum efficiency at 420 nm	20 %

Table 1: Parameter list of the fiber detectors for the FPS

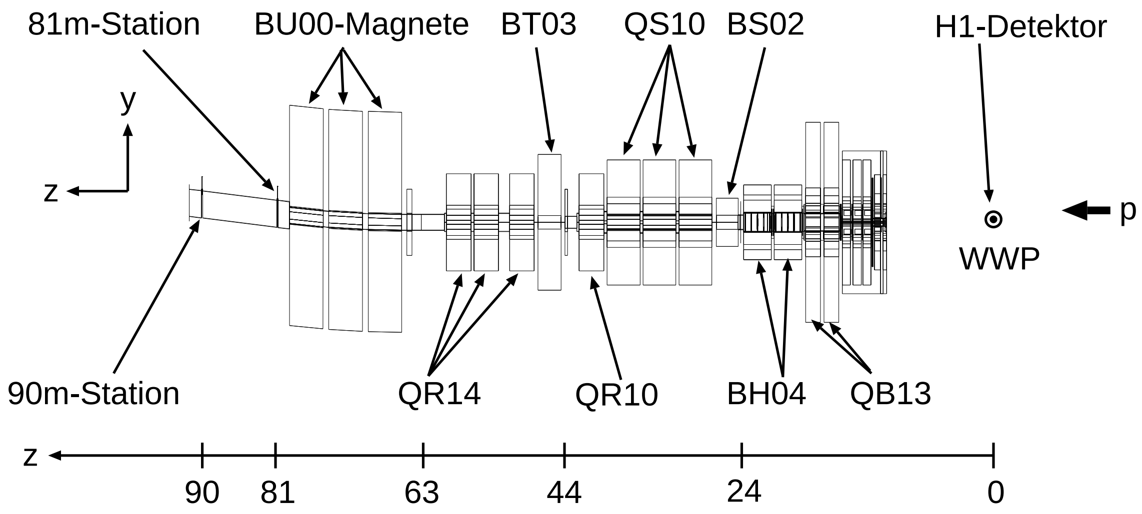

Figure 2: HERA–beam line adjacent to the H1 interaction region. The magnets BH04 introduce a horizontal bend, BU00 are vertical dipoles. Quadrupoles are QB, QB, and QS, correction coils are BT and BS, also shown is the position of the detector stations.

Observed rates	
Single tile rate 81 m	50 kHz
Single tile rate 90 m	20 kHz
Single pot trigger rate	5 kHz
Coincidence rate 81 / 90 m	1 kHz

Table 2: Observed counting rates in H1 luminosity runs.

photomultiplier (PSPM). The ambiguities are resolved by scintillator tiles in front and behind the hodoscopes, which also provide a trigger element to the general H1 trigger mix to signal a candidate particle passing through both stations. Some of the main detector parameters are summarised in table 1.

2.1 Performance of the FPS

When stable beam conditions are reached in a luminosity run the plunger vessels are moved into positions about 4 mm away from the circulating proton beam controlling the approach by monitoring a set of counting rates.

For typical proton currents of about 45 mA and 20 mA electron beams with both pots close to the beam, trigger tile single rates between 5 and 50 kHz are observed, well within the electronics capability, while the coincidence rate for three out of four trigger planes in each station is of the order of 2 kHz. The coincidence rate between the two stations is about 1 kHz. Table 2 summarises these rates in a comprehensive form.

The efficiencies of the scintillating fiber hodoscopes are inferred from the number of

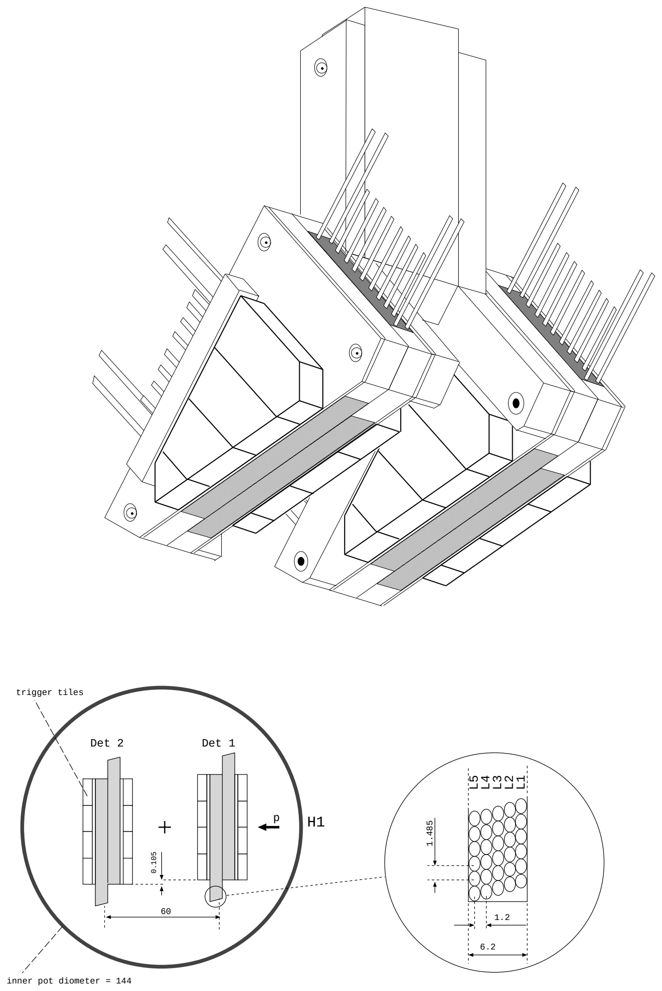

Figure 3: Perspective view of trigger tiles and scintillating fiber hodoscopes of a detector unit inside a Roman Pot. Below: Details of the scintillating fiber hodoscopes sandwiched between trigger tiles.

hits belonging to a track candidate. On average 6.5 hits per coordinate are observed in a layer of 10 scintillating fibers resulting in an average efficiency of 65%, which compares well with the geometrical efficiency. The observed spatial resolution of $\sigma_{xy} = 150$ μm is close to the design value.

In order to demonstrate the capability of the FPS trigger an event is shown in Fig. 4, which is a candidate for diffractive photoproduction with a proton seen in both stations at 80 and 90 m.

3 Momentum Analysis

The algorithm for momentum reconstruction relies on the fact that for particles originating at the interaction point there exists a one-to-one correspondence between the coordinates and slopes of trajectories at 85 m and energy and emission angle at origin. This statement may be inferred from the diagrams of Fig. 5, where for both coordinates (x horizontal and y vertical) the displacement with respect to the nominal orbit is plotted versus the slope measured at 85 m for trajectories starting at the the interaction point. Taking advantage of the dispersion in two planes enables two independent measurements

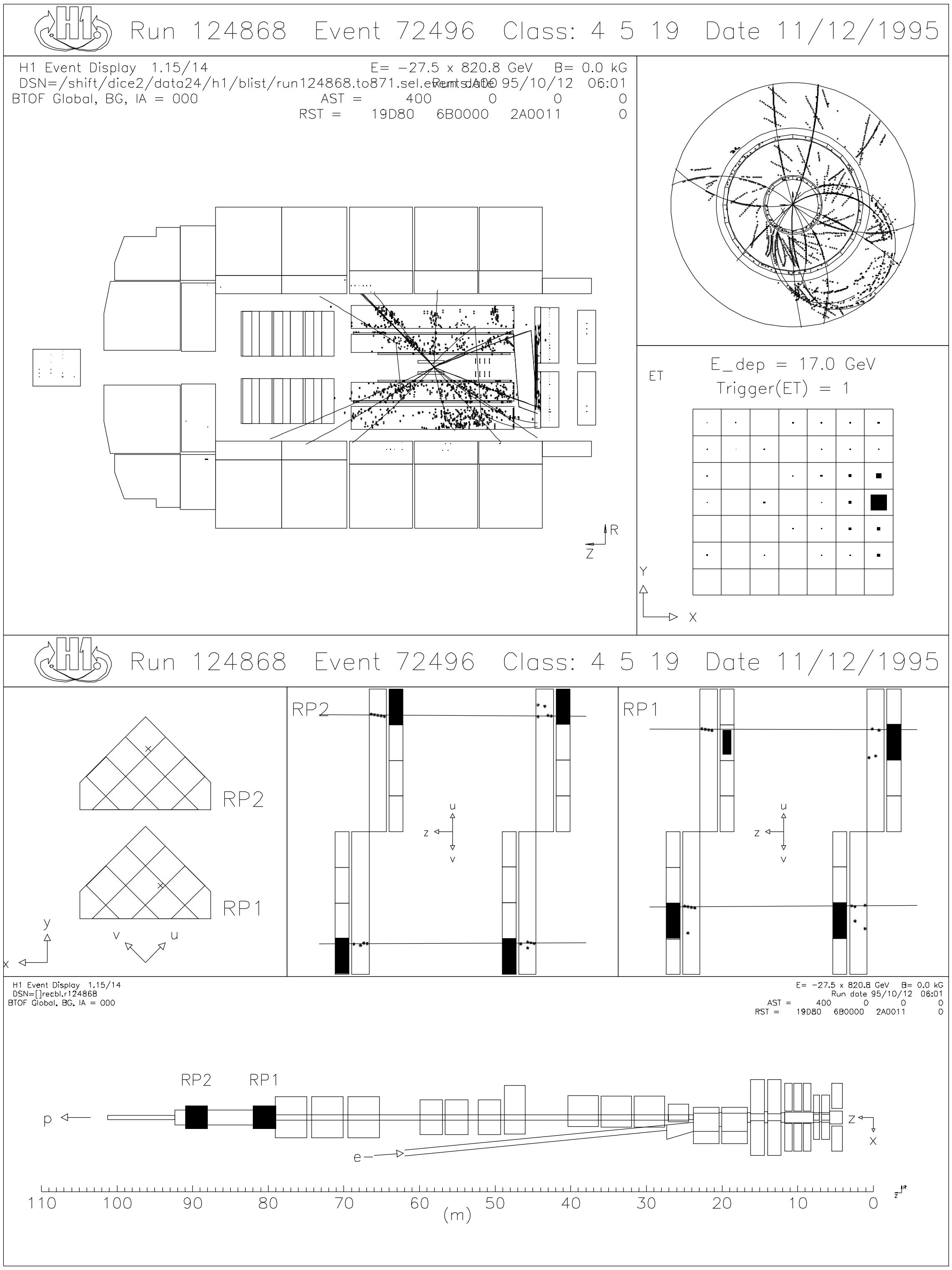

Figure 4: Tagged photo-production event with a track seen in both pots. In the upper half of the figure rz and rϕ projections of the central detector are shown as well as the signal of a tagged electron. The lower half shows hits in the trigger tiles of the 81 and 90 m detectors and the position of the hits in the fiber hodoscopes.

of longitudinal particle momenta, which have to agree within errors for genuine protons from ep interactions. This constraint is used in rejecting background tracks and improving on the momentum resolution. These plots also show that there are areas with densely packed trajectories which leads to a correspondingly bad momentum resolution.

3.1 Calibration

In order to reconstruct longitudinal momenta, all coordinates and slopes have to be measured with respect to the circulating beam. For this purpose the HERA beam position monitors are not sufficiently well calibrated. In particular their absolute position with respect to the H1 coordinate system are not known to better than 1 mm. Therefore a calibration method is used which relies exclusively on measured data inside the Roman Pots. Starting from nominal positions of the detector elements known from construction and from a survey in the HERA tunnel with respect to reference magnets of the proton machine, proton momenta and emission angles are reconstructed by applying the known beam optics transfer matrices of the spectrometer. These first order values are then corrected for the actual beam position.

The horizontal beam position is obtained by making use of the observation in Fig. 5 that all trajectories meet in one point in the (x,x') plane and that there are forbidden regions in this plane for particles starting at the interaction point. In a maximum likelihood fit the horizontal beam position is adjusted such that the expected pattern is optimized with respect to the observed one. The result of this procedure is displayed in Fig. 6b for one particular HERA fill. The zero order approximation to x and x' is shown in Fig. 6a. After adjusting the horizontal position and the horizontal slope of the proton beam, the distribution of Fig. 6b has only a very small number of entries in the forbidden region.

A similar procedure is applied for correcting the vertical position and slope. After having calibrated x and x', the vertical coordinates are obtained from a maximum likelihood fit, which in addition to the number of entries outside the allowed region minimizes the difference between the energies measured in the horizontal E_x and vertical planes E_y. The reason for using a different procedure for the y-coordinate may be inferred from Fig. 5b. There we observe that the allowed region in the y, y' plane is bounded only on one side such that an additional constraint is necessary to fix the scale for the emission angle. The result of such a fit can be inferred by comparing the plots of Fig. 6c and d.

With the method described above, an average momentum resolution of 4 GeV is achieved. More details are shown in Fig. 7. We observe a narrow correlation between the measurements in the two planes with a width of 5.9 GeV. As shown in Fig. 7b, the momentum resolution depends on the actual momentum, and from Fig. 7d, where the difference E_x - E_y normalised to the error is plotted, we learn that the errors assumed are reasonable, because the width of a Gaussian fitted to the experimental distribution has a width close to unity as expected.

Together with longitudinal momenta, the reconstruction through transfer matrices of the magnetic channel delivers values for the starting angles of trajectories at the interaction point. According to the diagrams of Fig. 5 the angular resolution in Θ_x is expected to be nearly independent of momentum in agreement with the experimental observation of a

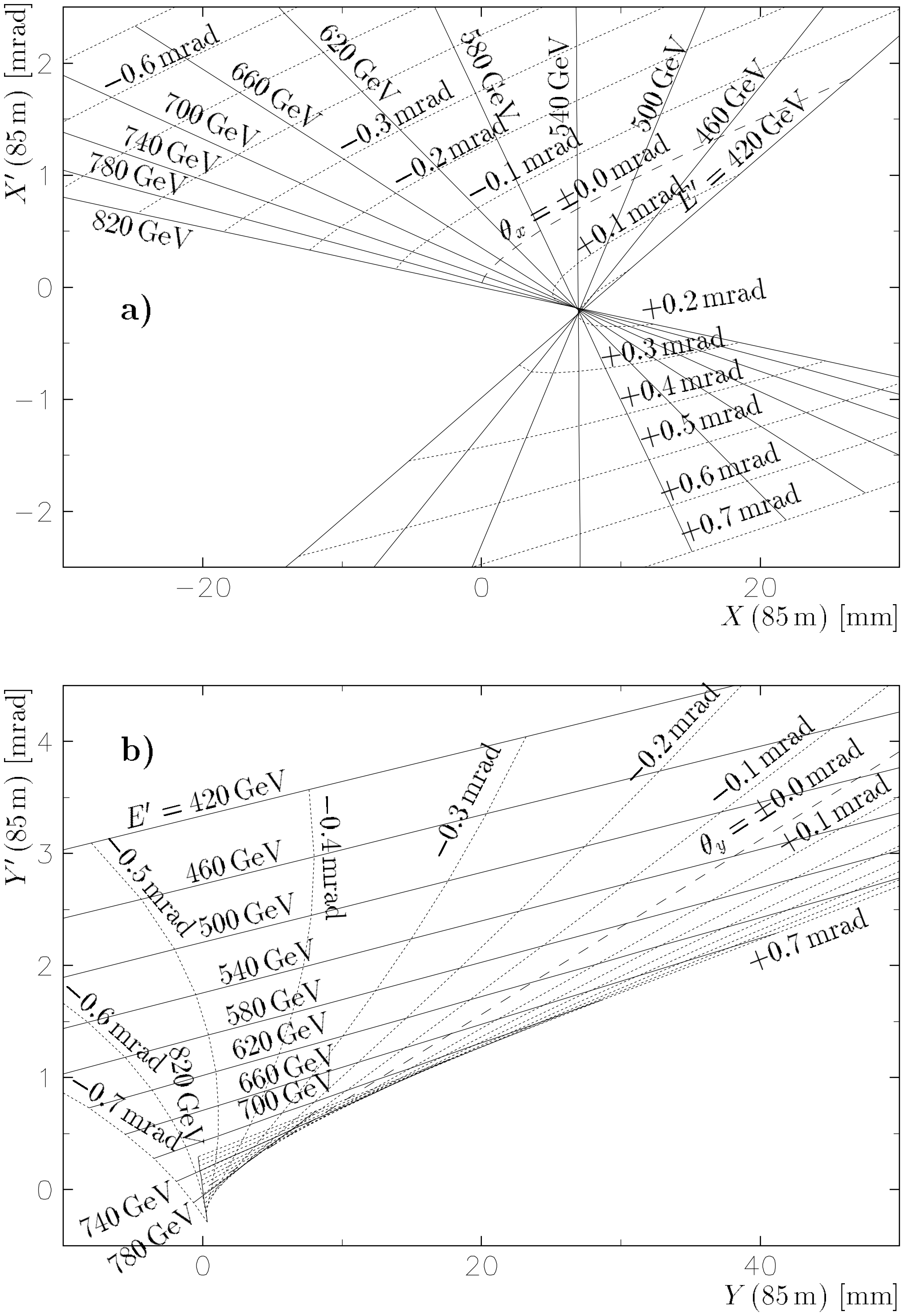

Figure 5: Dispersion at 85 m, displacements with respect to the nominal orbit (X, Y) versus the slopes (X', Y') in the horizontal (a) and vertical (b) plane for protons of different energies and emission angles.

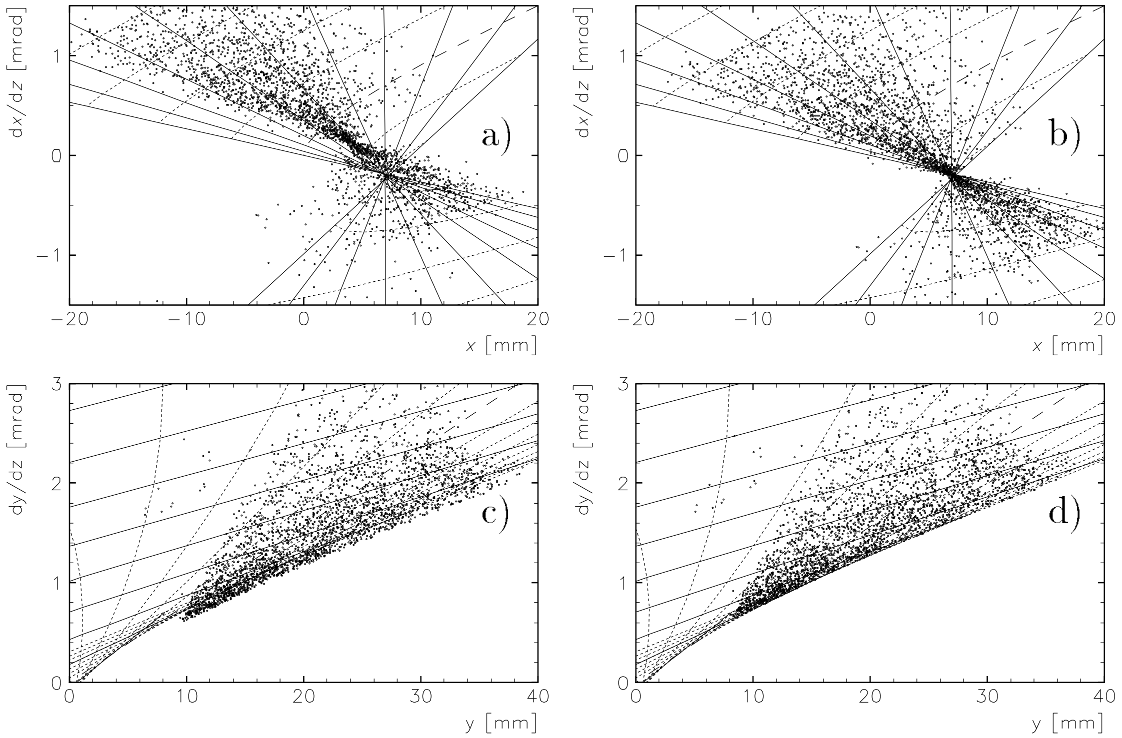

Figure 6: Calibration of the beam positions and slopes in two coordinates.
a) x vs. x' assuming nominal positions
b) x vs. x' after fitting the horizontal beam position and slope
c) y vs. y' assuming nominal positions
d) y vs. y' after x and y calibration.

constant value of $\sigma(\Theta_x) = 15\ \mu$rad much smaller than the natural beam divergence. The error on the vertical emission angle Θ_y is in contrast strongly correlated to the measured momentum receiving values of $\sigma(\Theta_y) \leq 100\ \mu$rad.

3.2 Momentum Reconstruction

The procedure outlined in the previous paragraph is used to calculate run dependent calibration constants. These are used to establish look up tables, which relate measured trajectory positions and slopes at 85 m to energies and emission angles at the interaction point. Using full error correlation matrices longitudinal momenta are quoted as weighted means of the independent measurements in the two planes.

As a first check of the method we use events from deep inelastic ep reactions in which all final state particles are recorded in the central H1 detector with the exception of the recoil proton to compare the observed missing longitudinal momentum with the one measured with the FPS. After cuts 6 events at $Q^2 \geq 100$ GeV^2 with a forward rapidity gap are left for such a comparison. These events are plotted in Fig. 8, where the missing longitudinal momenta reconstructed from the central H1 detector are compared with the momenta measured by the FPS. A clear correlation is seen between the two energies. This type of comparison with calorimeter data allows a first estimate of a systematic error of 3%.

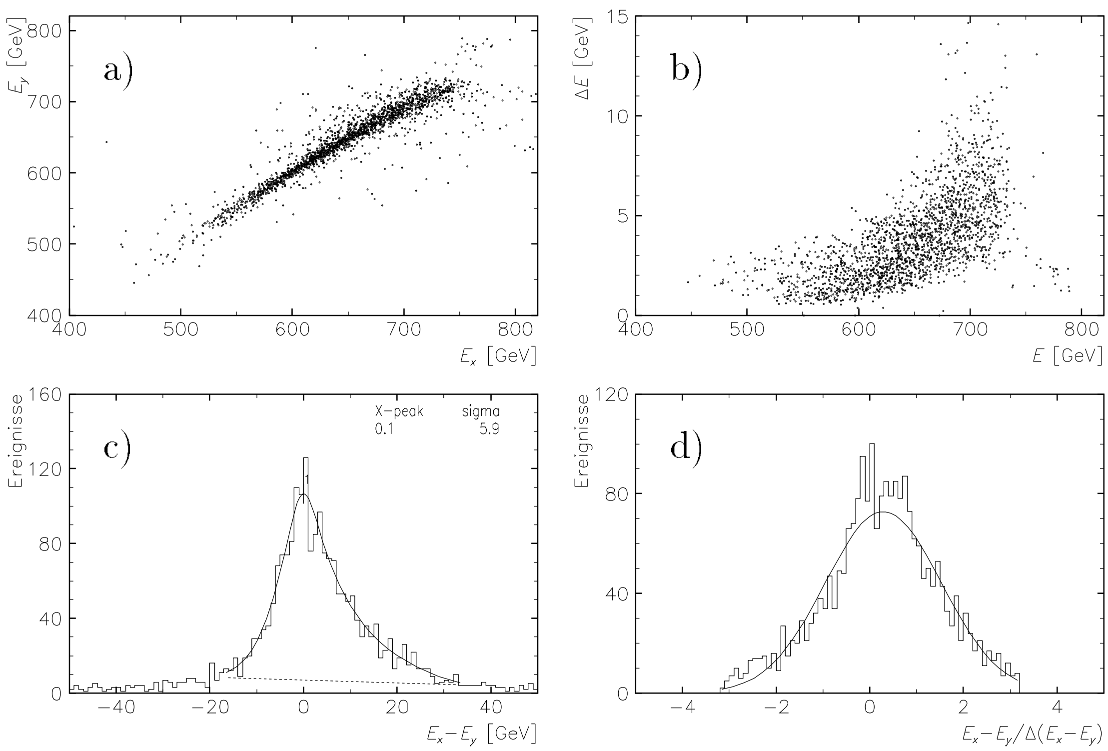

Figure 7: Momentum resolution for one proton fill.
a) compare energy measurements in X and Y
b) errors ΔE on the measured energy E
c) difference E_x - E_y
d) energy difference E_x - E_y normalised to the error $\sqrt{\Delta E_x^2 + \Delta E_y^2}$. The Gaussian fit has a mean value of 0.24 and $\sigma = 1.24$.

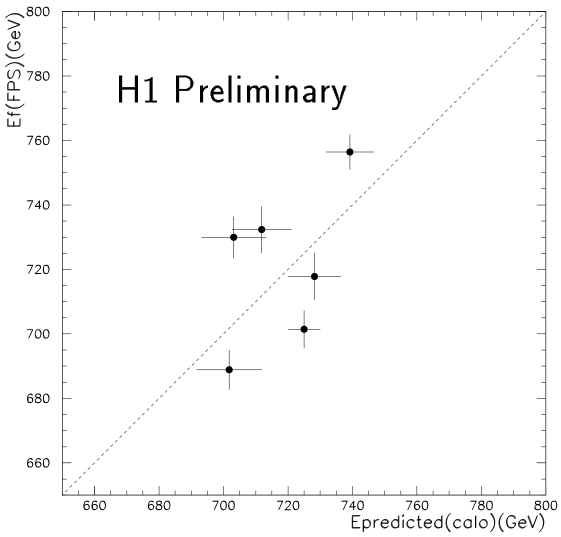

Figure 8: Comparison between the proton energy measured in the FPS and the missing longitudinal energy calculated from the calorimeter recordings in high Q^2 rapidity gap events.

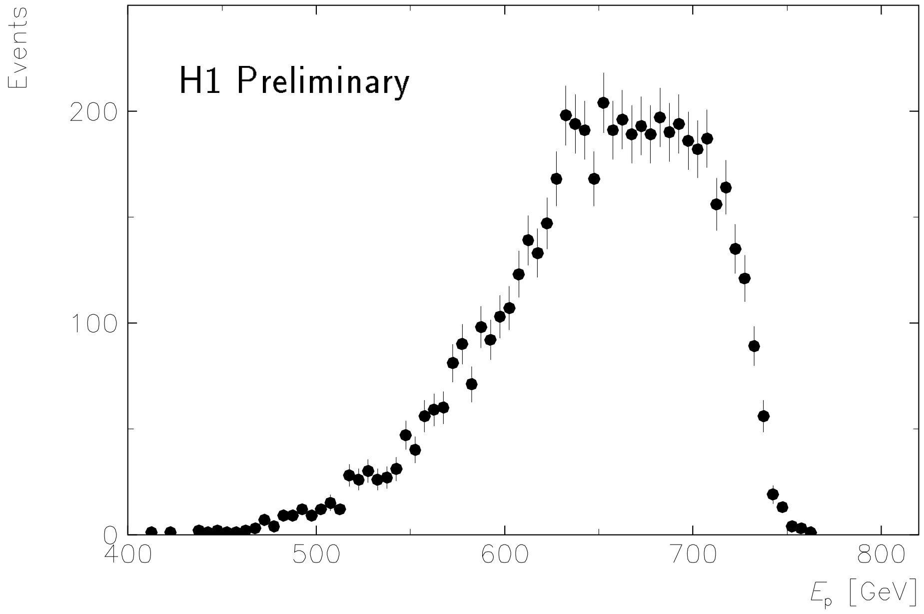

Figure 9: Energy spectrum of protons observed in DIS events with $1\,\mathrm{GeV}^2 < Q^2 < 100\,\mathrm{GeV}^2$. The shape of the spectrum is dominated by the energy dependent acceptance of the FPS.

An observed recoil proton spectrum from deep inelastic scattering at Q^2 below 100 GeV^2 is shown in Fig. 9. The shape of the observed spectrum is dominated by acceptance effects, which are not yet unfolded. The future physics analysis will concentrate on investigations into the nature of diffractive processes in deep inelastic scattering and photoproduction.

4 Conclusions

The forward proton spectrometer of H1 improves the physics scope of the experiment by providing a momentum measurement of forward going protons. The HERA beamline magnets are employed as a spectrometer which records scattered protons in two stations 81 and 90 m downstream the interaction point. Detectors with scintillating fiber hodoscopes for measuring two space points on a trajectory have proven to be robust instruments with a spatial resolution to provide a momentum resolution well below 1% with an overall scale uncertainty of 3%.

In a next step it is planned to upgrade the FPS by adding two more detector stations in order to improve the momentum coverage of the spectrometer. The new stations will employ the same technique as the old ones.

Acknowledgments

We are grateful to the HERA machine group whose outstanding efforts have made and continue to make this experiment possible. We thank the engineers and technicians for their work in constructing and now maintaining the H1 detector, our funding agencies for financial support, the DESY technical staff for continual assistance, and the DESY directorate for the hospitality which they extend to the non–DESY members of the collaboration.